Experiments with Global Detection of Cold Fusion Byproducts

Daniele GOZZI[‡], Pier Luigi CIGNINI[*], Riccarda CAPUTO[‡], Massimo TOMELLINI[#], Giovanni BALDUCCI[‡], Guido GIGLI[‡], Evaristo CISBANI[†°], Salvatore FRULLANI[†°], Franco GARIBALDI[†°], Mauro JODICE[†°] and Guido Maria URCIUOLI[†°]

ABSTRACT

On the line of the previous experiments carried out in a multicell electrochemical system, we will present the results obtained with an improved experimental apparatus recently assembled. In the present experimental configuration, we have a 60 ^{3}He tubes neutron counter from Jomar/Canberra (Los Alamos, NM) in which the ten cells system is located. In this way the efficiency of the neutron detection has been increased from 5×10^{-5} to 0.22. The sixty tubes are divided in twelve groups to localize which cell is generating neutrons owing to the counting of the twelve separated scalers. ^{4}He determination by mass-spectrometry is another feature recently added to our experiment.

Preliminary results confirm what we already obtained and presented at ACCF2 last year. They are essentially the production of excess heat up to 43% without any appreciable neutron and tritium excesses compared to the respective backgrounds. A carefull check of the neutron data, through the analysis and dating of the single pulse shape, is still in progress to identify if intense spikes observed in the R+A count are due to a real *in situ* nuclear phenomena or background or artifact effects.

[‡]Dipartimento di Chimica, Università La.Sapienza, P.le Aldo Moro 5, 00185 Roma
[†]Laboratorio di Fisica, Istituto Superiore di Sanità, V.le Regina Margherita 299, 00161 Roma
[°]INFN sez.Sanità, V.le Regina Margherita 299, 00161 Roma
[*]CNR-Centro di Termodinamica Chimica alle Alte Temperature, c/o Dipartimento di Chimica, Università *La Sapienza*
[#]Dipartimento di Scienze e Tecnologie Chimiche, Università Tor Vergata, 00100 Roma

FRONTIERS OF COLD FUSION

1. Introduction

Since 1989 the activity on *cold fusion* is mostly oriented to understand the true nature of the observed phenomena: if they are due to artifacts and/or known chemical and physical effects or they belong to a category of new phenomena which open a very interesting window in the physics of the condensed matter.

The continuous improvement done on our experimental set-up is a clear evidence that our activity follows this guideline. In this framework, we moved and are still moving to design an experiment in which as many as possible independent variables can be measured *in situ* and at the same time in a multicell F&P-like experiments.

Aim of this contribution is to show our recent results obtained in an improved experimental set-up which has been modified expecially in the parts of neutron detection and treatment of electrolysis gases before sampling for ^4He mass-spectrometric determination.

2. Methods

We will limit to describe only the parts which were changed or added with respect to our previous experiments reported in literature[1-2].

The flow-chart characterizing each cell is reported in figure 1 below.

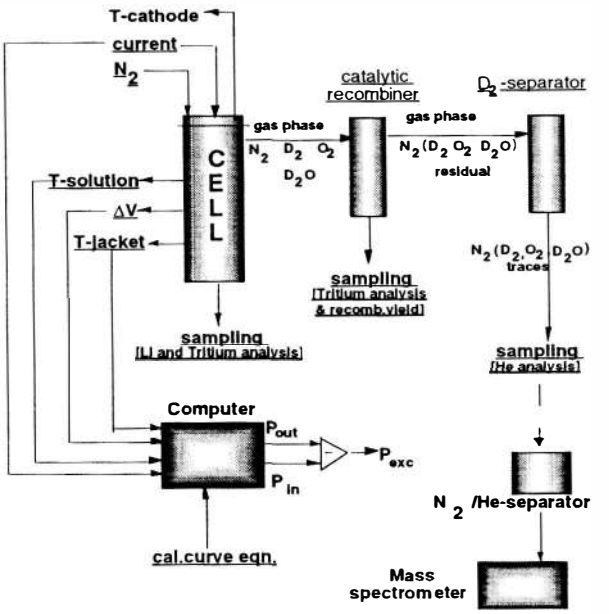

Figure 1. Flow-chart of one cell apparatus.

Electrochemical Cells

Heat excess is measured in a non-adiabatic calorimeter-electrochemical cell through the comparison with the thermal and electrochemical calibration curves obtained, using Au or Pt cathodes, in the same experimental conditions in which the experiment is then carried out. Cell geometry and carrier gas bubble stirring allow to

take into consideration only the thermal gradient on the plane orthogonal to the z-axis, so the calibration curve, obtained as a sequence of stationary states at constant input power values, P_{in}, is linear according to equation $\Delta T = P_{in}/k$. $\Delta T = T_s - T_j$ and T_j is the temperature of the thermostated water circulating in the torus-shaped bath. The heat excess is given by $P_{exc} = P_{out} - P_{in} = k\Delta T - P_{in}$ where ΔT is now the value measured in the experiment.

Features of such cells as calorimeters are:

- Materials- body: glass, cap: teflon
- Dimensions- inner ø 22 mm x 245 mm height
- Minimum heat detectable: 0.5 ÷ 1 W
- Maximum Input Power: 50 W
- Time constant: ≈ 350 s
- Continuously fluxed under N_2 (from LN_2) at controlled flow-rate

Features as electrochemical cells are:

- Electrolytic solution: 0.2 M LiOD(LiOH) in $D_2O(H_2O)$
- Anodes: Pt wire ø1mm shaped as cylindrical coil (10 mm inner ø x 20 mm height)
- Cathodes: pure Pd centered in the z-axis of anode. Mostly shaped as ø3mm rods subjected to different thermal and/or mechanical treatments according to the procedures indicated below:

A.Heated under $1x10^{-6}$ mbar at 1050 °C for 24 h and cooled at 0.5 °C/min
B.Screw dislocated by 3 rotations at room temperature
C.Screw dislocated by 3 rotations in LN_2
D.Screw dislocated (0.5 mm ø wires) by 11 rotations at room temperature
E.As received
F.Edge dislocated under 10^4 kg for 15 h at room temperature
G.Edge dislocated under 10^4 kg for 30 min in LN_2

Table 1 shows some characteristics of the cathodes used in the experiment here reported. Cells #1 and #8 were used as blanks; the first one had a Au cathode and in the second one the electolytic solution was LiOH in H_2O. Figure 2 shows, as typical, the calibration curves obtained both in thermal and electrochemical mode. As

Table 1. Characteristics of the cathodes

# Cell	Dimensions/mm ø x h	S.Area to Volume Ratio/cm^{-1}	Treatment& material
1	3 x 31	13.6	E&Au
3	3 x 28	13.7	AC&Pd
5	0.5 x 28*	8.1	D&Pd
7	3 x 30	13.7	EC&Pd
8	3 x 30	13.7	A&Pd
9	3 x 26**	10.0	F&Pd

*23 wires gold-soldered at one end to form a single cathode
**Starting dimensions of the road. After treatment F, dimensions were 6x1 (thick) x 26(height)

already discussed[2], in principle, both the calibration curves should be superimposed. Slight differences can be observed due to the different location in the cell of the heat sources (heater in the thermal mode, electrodes in the electrochemical one). Each cell indicated in Table 1 was calibrated in both the modes and in all the cases straight lines, $\Delta T_i=(a_i\pm\Delta a_i)+(b_i\pm\Delta b_i)P_{in}$, were obtained.

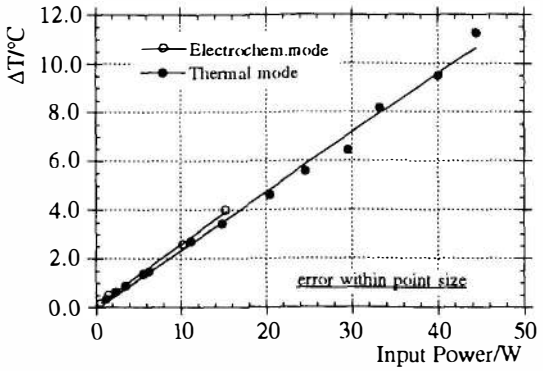

Figure 2. Typical calibration curves obtained in thermal and electrochemical mode

In Table 2, the averaged coeffients between the two modes were reported for each cell.

Table 2. Coefficients of the calibration curve equations

#Cell	$(a_i \pm \Delta a_i)$/°C	$(b_i \pm \Delta b_i)$/°CW^{-1}	R
1	0.05±0.06	0.128±0.004	0.9982
3	0.02±0.05	0.213±0.002	0.9996
5	-0.04±0.09	0.250±0.007	0.9977
7	-0.02±0.07	0.228±0.004	0.9977
8	0.08±0.02	0.297±0.001	0.9998
9	0.09±0.02	0.299±0.001	0.9999

^{4}He Detection Procedure by Mass-Spectrometry

In this section details are given for a procedure which is under development in order to detect ^{4}He in electrolysis gases. Present data refer to synthetic mixtures modelling the expected ones. The Mass Spectrometer used is a Nuclide Analysis Associates HT 7 (60°,12" radius) equipped with an electron impact ionization source and a sixteen stages Cu/Be electron multiplier. The Knudsen cell molecular source has been removed and replaced with a flange carrying an inlet system *via* a Balzers UDV 235 gas valve. The sample gas flows through the valve and a quarz tubing inserted into the ion source; the resulting flux is colinear to the ion path. The typical settings of the mass spectrometer main parameters are:

- electron ionization energy 100 eV
- electron emission current 1.0 mA
- ion accelerating potential 4510 V
- electron multiplier gain (mass 28) 2.0×10^5

For a given mass spectrometer, sensitivity is mainly affected by, on one hand, the partial pressure of ^{4}He realized in the ionization chamber and, on the other hand, the resolving power needed in order to discriminate between D_2 and ^{4}He peaks. A compromise must be reached. Indeed high partial pressures of ^{4}He admitted to the mass spectrometer imply, due to N_2 and D_2 in the carrying gas, an overall high pressure in the ionization chamber. As a consequence broadening of the mass peaks occurs. This requires an increase of the resolution to be used which, in turn, reduces the mass spectrometer sensitivity.

Neutron detector

A new high efficiency neutron detector has been used in the present experiment. It has been designed and manufactured, according to our specifications, by Jomar Systems Division of Canberra Industries Inc. Its design derives from detectors developed for the passive assay of plutonium in solid waste drums through non-destructive measurement system[3] in the advanced version used by H. Menlove also for cold-fusion experiments[4]. Complete description of the detector with its performances, experimental results and Monte Carlo simulations will be reported in a paper in preparation; here we summarize the main characteristics. The new neutron detector consists of 60 ^{3}He-proportional tubes of 41 cm active length, 2.54 cm diameter and 6 atm gas pressure. These tubes are embedded in a cylindrical polyethylene moderator. The detector is segmented in twelve independent counters consisting of five tubes each, arranged in inner and outer rings of six counters. The positions of the central tubes of each counter are stacked of half counter length between the inner and outer ring (see Fig. 3). The torus containing the ten electrochemical cells is surrounded by the detector and the localisation of the cell at the origin of the neutron emission can be obtained through the analysis of the pattern of the counts registered by the different twelve counters.

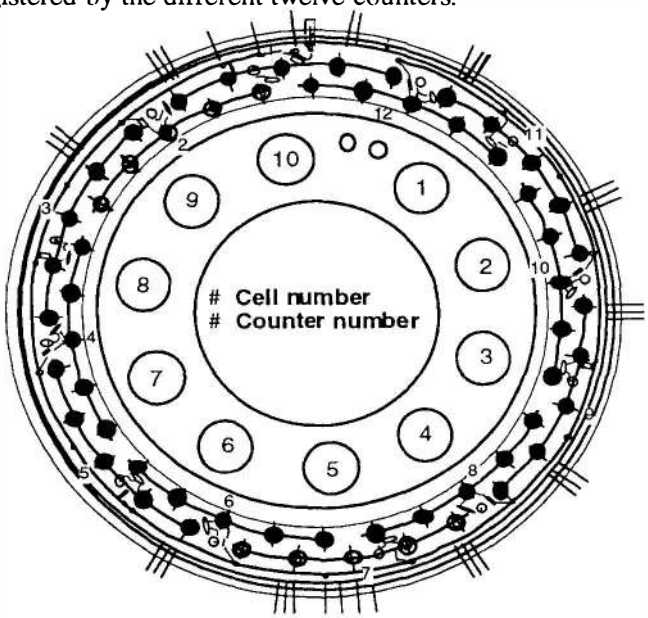

Figure 3. Neutron detector. Location of counters and cells.

If the emission is burst-like, the time correlated counts (with time correlation consistent with the die-away time of the detector) should affect contiguous numbered counters of the inner and outer rings facing the cell where the emission has occurred.

The efficiency of the detector measured with a source of Californium-252 placed in the different positions of the ten cells is 22%. The dependence of the efficiency on the cell position is limited to less than 1%. The counts are essentially distributed among three or four contiguous numbered counters shared between inner and outer rings. This distribution should allow the identification of the emitting cell if bursts of neutrons occur or if random generated emissions of neutrons happen at a

rate substantially higher than the background. In the present conditions of the experiment the background of the whole detector is about 1 count/s that means about 0.3 counts/s in a group of four contiguous numbered counters. The signals from eacl group of five tubes are processed by an AMPTEK A-111 hybrid charge-sensitive pre-amplifier/discriminator[5] that gives then, as output of the counter, both the digital and the linear OR of the five tubes. The scheme of the electronics used to derive and acquire the information from the detector is shown in Fig. 4. Digital output of each counter is sent to two scaler one of which is read and reset at fixed time interval and the other is read and reset only at the end of a run lasting several days.

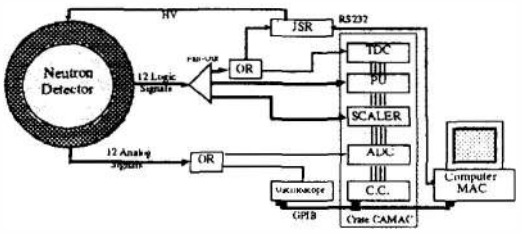

Figure 4. Simplified scheme of neutron detector electronics

In parallel it is sent to a Pattern Unit in order to detect all the counters hired within the time allowed by the acquisition cycle time (at present of the order of 1 ms) Moreover it is used to have a logical OR of all the twelve counters. The logical OR is elaborated in order to measure with a TDC, for each neutron detected, the time interval between it and the following one. The logical OR is also sent to the Jomar JSR-12 Neutron Coincidence Analyzer[6]. The main purpose of the JSR-12 is to act as a filter in order to enhance the capability of detecting time-correlated counts through its scaler R. In fact, each time a neutron is detected, a scaler T (Total) is incremented by a single count and two intervals of time are opened. the first one starting few μs after the detection and the second after about 1 ms. In the first gate both random neutrons and neutrons correlated with that one that has allowed the gate to be opened are expected, while in the second gate only random neutrons are waited due to the large interval of time elapsed in respect to the die-away time of the detector. The counts in the first gate increment in non-linear way the R+A (Real + Accidentals) scaler of JSR-12; while those in the second one increment the A scaler. The two gate are opened for each neutron detected, then the increment of R+A is equal to the sum of the neutrons detected in each opened gate. When N neutrons are emitted in a very short time interval and all detected within the time interval of a single gate, the increment of the R+A scaler is equal to N(N-1)/2. The comparison of R+A and A scalers allows to estimate the number of correlated neutrons. The background value of this R+A scaler during the experiment was about 0.5/min, i.e., about a factor hundred less than the background value of total counter T. These counts are due essentially to cosmic rays spallation neutrons. The background value of the A scaler was a factor hundred less than the R+A value.

The twelve analogic signals from the twelve counters are amplified and then sent to a linear fan in-fan out from which two linear OR of these signals come out. The first one goes to a wave form digitizer, a digital oscilloscope, which permits to acquire the information on each pulse including the absolute time (given with a precision of ns) and the wave form; the second goes to an ADC that digitizes its integral and sends the value obtained directly to a histogramming memory. Scaler , pattern unit, TDC, ADC and histogramming memory are CAMAC modules and are

read through CAMAC BUS by a crate controller driven by a Macintosh II personal computer through a GPIB IEEE port that drives also the oscilloscope. The computer reads the pattern unit at each occurrence of CAMAC Look At Me (LAM) signal and reads the histogramming memory and the scalers each ten minutes. The (LAM) signal is emitted when the pattern unit has received at least one logic pulse from the detector. Besides, in order to minimize the time spent in readout, the computer does not read the oscilloscope until this has acquired a fixed number of pulses (block). This number is limited by the storing capability of the oscilloscope and depends on the choice of the number of points by which the pulse is digitized. Typical figures are: 100 points for each pulse and 1000 waveforms/block acquired before the computer reads the oscilloscope.

3. Results

Calorimetry

In order to give a synthetic view of the calorimetric data, we will use Table 3 to summarize the results obtained in all the cells and the related plots, assumed as typical, will be shown only for cell #5.

During the experiment, lasted more than 650 h, the current applied to the cells, which are connected in series, was changed both in step-fashion and modulated high-low according to a square-wave.

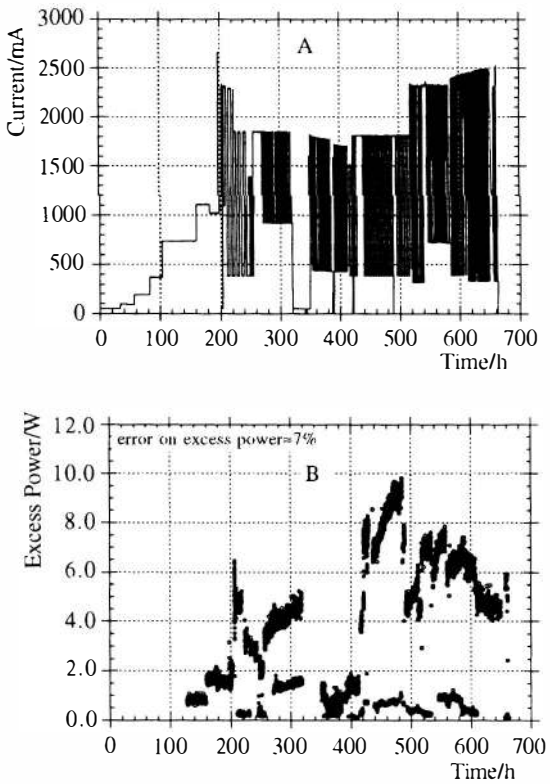

Figure 5. A. Profile of the current throughout the experiment. B. Excess power measured on cell #5.

Figure 5 shows the profile of the current applied to the cells and the measured excess power (cell #5) throughout the entire experiment.

The same excess power reported in fig. 5 is correlated with the input power in figure 6 below. In the same figure, the inset gives the ΔT trend with respect to the same power input range.

In Table 3 below, the integrated heat, Q, is calculated for 535 h where the heat production was at sufficient rate. The column, $(P_{exc}/P_{in})\%$, has to be intended as the maximum yield found and, in column P_{in}, the corresponding input power. For cells #1 and #8 any appreciable excess power was found.

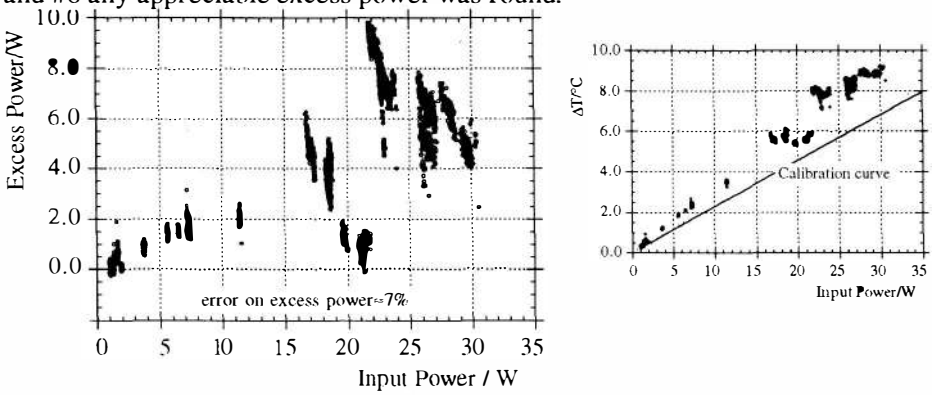

Figure 6. Excess power as a function of input power, P_{in}, at cell #5. In the inset, $\Delta T=T_S-T_j$ *vs* P_{in} compared with the calibration curve of cell #5.

Table 3. Summary of excess data found

#Cell	$(P_{exc}/P_{in})\%$	P_{in}/W	Q/MJ
1	-	-	-
3	32.2 ± 0.2	25	4.0
5	43.3 ± 0.4	22	6.0
7	42 ± 1	20	4.3
8	-	-	-
9	38 ± 1	21	3.1

$^4He/D_2$ separation tests

At present, the best sensitivity has been attained by valving off pumping in the ionization region; pressure in this region, during measurement, was $4x10^{-5}$ mbar . Typical resolution used, as from the half height measurement, is $M/\Delta M = 930$. Attempts are currently being made in order to increase the ratio between ^4He and the other gases admitted to the mass spectrometer by employing selective membranes. Recent data confirm that our procedure allows to eliminate D_2 from the electrolysis gas mixture at least in the limit of the mass spectrometer resolution. More details will be given in a paper in preparation.

Tritium measurements

As reported elsewhere[1,2], our procedure allows to determine tritium both in the solution and in recombined gases. Figure 7 shows both the trends throughout the

experiment. To compare with respect to electrolytic enrichment, data are plotted against the charged, ∫Idt, passed through the cell at time t.

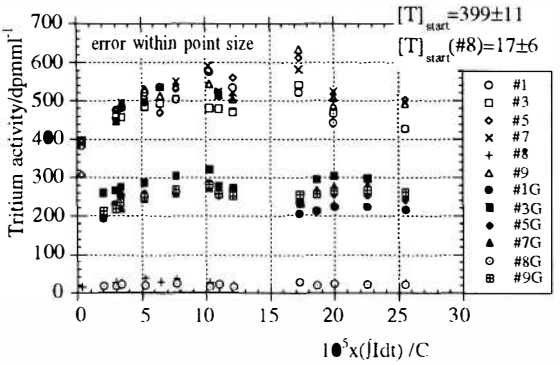

Figure 7. Tritium activity as measured throughout the experiment. Lower points correspond to the activity measured in recombined gases.

Neutron measurements

The analysis of all the information acquired during the experiment is still in progress. No evidence of neutron emission has been found in the analysis of the total counts integrated in 10 minutes time intervals. Even if our background level is very high, we can exclude the occurrence in the present experiment of events generating flux of thousands neutrons per second, seen in some previous experiment, lasting even few seconds.

The analysis of the correlated neutron events (R scaler) with the parallel analysis of the pulses wave form has shown the occurrence of several events whose pulse lasts for several hundreds of μs with overlapping of pulses and which give a big increment of the R scaler. The characterization of such anomalous events is still underway, aiming to check the digitized waveform of all the pulses acquired during all the ten minutes time intervals in which a value of R different from the background value has been found. Such analysis is extended also to characterize sporadic events occurred during the background acquisition with abnormal R scaler increment, in order to asses or reject a possible different nature between the events occurring when the electrolysis process is active from those occurring when the process is stopped.

4. Discussion

We briefly discuss the main aspects emerging from the above results. A more detailed discussion will be given elsewhere. Concerning the heat excess, we observe that we found, in a quite reproducible way with respect to our previous findings[2], a strict correlation of heat excess from the applied input power. As it appears from Fig. 6, the excess power is an increasing function of the input power. This behaviour is broken all the times the current is set to zero (see also Fig. 5). This seems to be in agreement with the hypotheses that *cold fusion* is feasible only if the D/Pd ratio is above a certain critical value and the loading of Pd by D is a process occurring under a gradient of electrochemical potential, as already pointed out in literature[7]. We can also observe that the maximum value of the excess power yield is located in the input power range from 20 to 25 W (see Table 3) and this is associated both to the

maximum excess power and a given current modulation, as reported for cell #5, in fig.5A,B. In fact, from the same figure, we can observe that excess power is particularly enhanced from the period of the current modulation instead of its amplitude. This is consistent with D diffusion time into Pd, $\approx x^2/d$ ($x=\phi/2$ in our samples, d=diffusion coefficient). Therefore, in the procedure adopted, we obtained that the maximum of excess power as well as the maximum ΔT did not correspond to the maximum value of the input power. This, if further confirmed, seems to be promising to develop the principles for practical applications of the *cold fusion.*

Concerning the production of nuclear particles, the present preliminary results seems to confirm both our previous results[2] and the general trend of *cold fusion experiments in which the nuclear particles are not systematically observed* as expected by the scheme of the plasma fusion reactions, if compared to the excess heat found. This is still the main question to which a satisfactory answer has not yet given. As shown in this Conference and in literature further experiments are still needed to confirm ^4He production associated to the excess heat. Our efforts are also oriented to give contributions accordingly.

Acknowledgments

The authors gratefully acknowledge the technical support of F. Giuliani, M. Gricia, M. Lucentini, L. Pierangeli and F. Santavenere of the Physics Laboratory of the Istituto Superiore di Sanità and INFN-Sanità and G. Gervasoni and S. Simonetti of the Department of Chemistry and CNR-Centro di Termodinamica Chimica alle Alte Temperature. The skill of M. Sabatini (Physics Laboratory of the Istituto Superiore di Sanità) in computer preparing drawings and materials for the poster presentation has been also of invaluable help.

References

1. Gozzi D. et al., 1992, J.Fusion Technology, 21, 60
2. Gozzi D. et al., Multicell Experiments for Searching Time-Related Events in Cold Fusion, Proc. 2nd Int. Conference on Cold Fusion, Villa Olmo, Como, June 29 - July 4, 1991, 1991, Conference Proceedings 33, 21, Società Italiana di Fisica, Bologna
3. Birkhoff G., Bondar L., Ley J., Berg R., Swennen R., Busca G., " On the Determination of the Pu-240 in Solid Waste Containers by Spontaneous Fission Neutron Measurements. Application to Reprocessing Plant Waste." Joint Nuclear Research Center Ispra Establishement, 1975, EUR 5158e; Bohnel K., "Die Plutoniumbestimmung in Kerbrennstoffen mit der Neutronen Koinzidenzmethode." Kernfoschungzentrum Karlsruhe, 1975, KfK 2203
   Krick M.S. and Menlove H.O., "The High-Level Neutron Coincidence Counter (HLNCC): User's Manual." Los Alamos Scientific Laboratory, 1979 LA-7779-M
4. Menlove H.O. and Miller M.C., 1990, Nucl.Instr. and Meth. A299, 10
5. Swansen J.E., 1985, Nucl.Instr.and Meth. B9, 80
6. Swansen J.E., Collinsworth P.R. and Krick M.S., 1980, Nucl.Instr.and Meth. , 176, 555; Menlove H.O. and Swansen J.E., Nucl.Techn. 71, 497
7. Tomellini M. and Gozzi D., 1990, J. Materials Science Lett., 9, 836